

GelSlim: A High-Resolution, Compact, Robust, and Calibrated Tactile-sensing Finger

Elliott Donlon, Siyuan Dong, Melody Liu, Jianhua Li, Edward Adelson and Alberto Rodriguez
Massachusetts Institute of Technology

Abstract—This work describes the development of a high-resolution tactile-sensing finger for robot grasping. This finger, inspired by previous GelSight sensing techniques, features an integration that is slimmer, more robust, and with more homogeneous output than previous vision-based tactile sensors.

To achieve a compact integration, we redesign the optical path from illumination source to camera by combining light guides and an arrangement of mirror reflections. The optical path can be parametrized with geometric design variables and we describe the tradeoffs between the thickness of the finger, the depth of field of the camera, and the size of the tactile sensing pad.

The sensor can sustain the wear from continuous use—and abuse—in grasping tasks by combining tougher materials for the compliant soft gel, a textured fabric skin, a structurally rigid body, and a calibration process that ensures homogeneous illumination and contrast of the tactile images during use. Finally, we evaluate the sensor’s durability along four metrics that capture the signal quality during more than 3000 grasping experiments.

I. INTRODUCTION

Tight integration of sensing hardware and control is the key to a human’s mastery of manipulation in cluttered, occluded, or dynamic environments. Artificial tactile sensors, however, are challenging to integrate and maintain: They are most useful when located at the distal end of the manipulation chain (where space is tight); they are subject to high-forces and wear (which reduces their life span or requires tedious maintenance procedures); and they require instrumentation capable of routing and processing high-bandwidth data.

Among the many tactile sensing technologies developed in the last few decades [1], vision-based tactile sensors are a promising variant. They provide high spatial resolution with compact instrumentation, and have interesting synergies with recent image-based deep learning techniques. Despite their unique capabilities, current implementations of these sensors are often bulky and/or fragile [2], [3], [4]. Robotic grasping benefits from sensors that are compactly-integrated and that are rugged enough to sustain the continuous shear and normal forces involved in grasping.

To address this need, we have developed a tactile-sensing finger, *GelSlim*, designed for the requirements of grasping

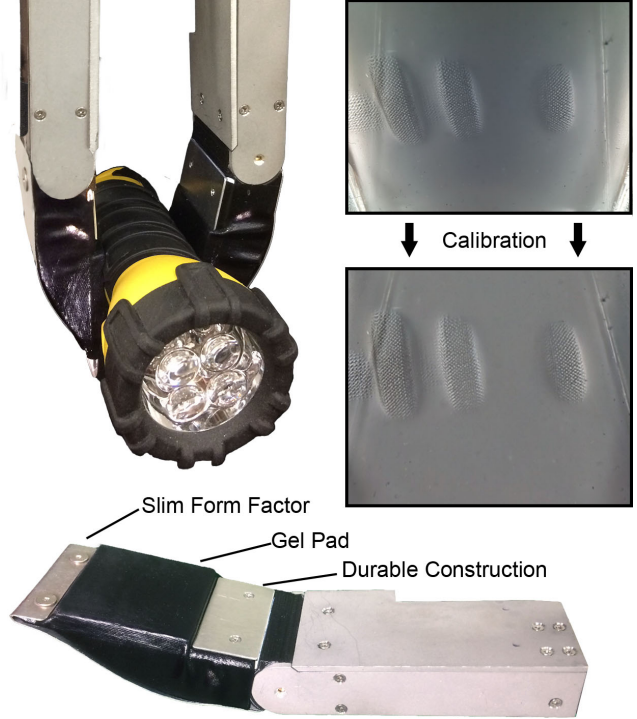


Fig. 1. **GelSlim** fingers grasping a textured flashlight with the corresponding tactile image at right. The sensor is calibrated to normalize output over time and reduce the effects of wear on signal quality. The finger, featuring a pointed adaptation of the GelSight sensor, is shown at bottom.

in cluttered environments (Fig. 1). This finger, like other vision-based tactile sensors, uses a camera to measure tactile imprints of objects like those seen in Fig. 2.

In this work we present:

- **Design** of a vision-based high-resolution tactile-sensing finger with the form factor and toughness necessary to sustain the normal and shear forces involved in everyday grasping (Section IV).
- **Calibration** framework to regularize the sensor output across time and individual sensors (Section V). In particular we suggest four metrics to track the quality of the tactile feedback.
- **Evaluation** of the sensor’s durability by monitoring its image quality over more than 3000 thousand grasps (Section V).

The long term goal of our research is to enable reactive grasping and manipulation. We believe that the use of tactile feedback in the control loop of a robotic manipulation system

Corresponding author: Elliott Donlon, <edonlon@mit.edu>.

This work was supported by the Karl Chang Innovation Fund, ABB, and the Toyota Research Institute.

The authors would like to thank Wenzhen Yuan for her expertise in making gels and willingness to teach; Francois Hogan, Maria Bauza, and Oleguer Canal for their use of the sensor and feedback along the way. Thanks also to Rachel Holladay for her totally awesome paper feedback.

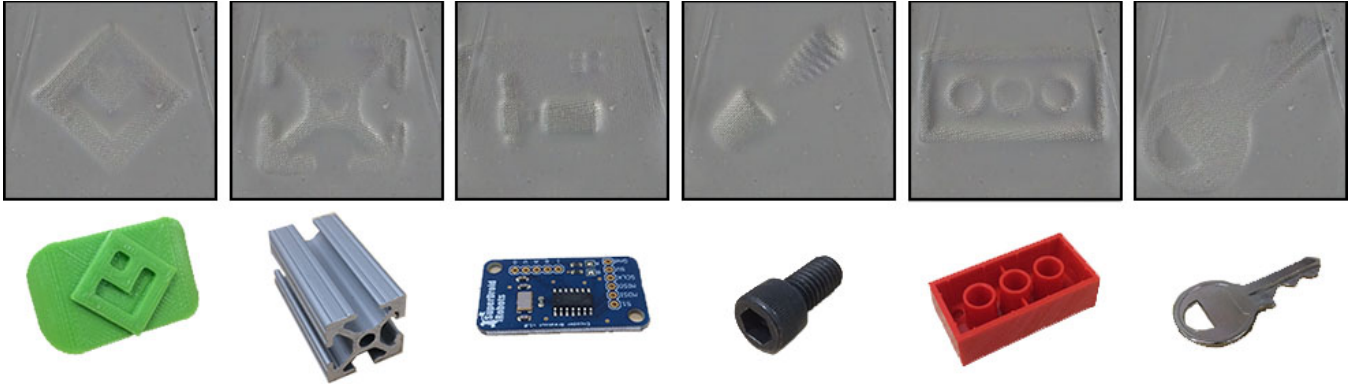


Fig. 2. **Tactile imprints** of objects around the lab. From left to right: The MCube Lab’s logo, 80/20, a PCB, a screw, a Lego brick, and a key.

is key for reliability. Our motivation stems from efforts in developing bin-picking systems to grasp novel objects in cluttered and partially observed scenes.

In cluttered environments like a pantry or a warehouse storage cell, as in the Amazon Robotics Challenge [5], [6], [7], a robot faces the challenge of singulating target objects from a tightly-packed collection of items. In these, and similar day-to-day tasks, cramped spaces and clutter lead to frequent contact with non-target objects. Fingers must be compact and, when possible, pointed to squeeze between target and clutter. To make use of learning approaches, tactile sensors must also be resilient to the wear and abuse from long experimental sessions which, especially while learning, yield unexpected collisions. Finally, we believe that sensor calibration and signal conditioning are key to improving the consistency of tactile feedback as the sensor’s physical components decay.

II. RELATED WORK

The body of literature on tactile sensing technologies is expansive [1], [8]. Here we discuss relevant works related to the technologies used by the proposed sensor: vision-based tactile sensors, and GelSight sensors.

A. Vision-based tactile sensors

Cameras provide high-spatial-resolution 2D signals without the need for many wires. Their sensing field and working distance can also be tuned with an optical lens. For these reasons, cameras are an interesting alternative to several other sensing technologies which tend to have higher temporal bandwidth but more limited spatial resolution.

Ohka *et al.* [9] designed one of the early vision-based tactile sensors in 1996. It is comprised of a flat rubber sheet, an acrylic plate and a CCD camera to measure three-dimensional force. The prototyped sensor, however, was too large to be realistically integrated in a practical end-effector. A human finger shaped tactile sensor called Gelforce [10] used a camera to track two layers of dots on the sensor surface, to measure both the magnitude and direction of an applied force.

Instead of measuring force, some vision-based tactile sensors focus on measuring geometry, such as edges, texture

or 3D shape of the contact surface. In 2000, Ferrier and Brockett [11] proposed an algorithm to reconstruct the 3D surface by analyzing the distribution of the deformation of a set of markers on their tactile sensor. This principle has inspired several other sensors. The TacTip sensor [2] uses similar principle to detect the edges and estimate the rough 3D geometry of the contact surface. Mounted on the GR2 gripper, the sensor was demonstrated to give helpful feedback when reorientating a cylindrical object in hand [12]. Yamaguchi [13] built a tactile sensor with a clear silicone gel that can be mounted on a Baxter hand. Different from the previous sensors, Yamaguchi’s also captures the local color and shape information since the sensing region is transparent. The sensor was demonstrated to be useful for detecting slip and estimating contact force.

B. GelSight sensors

The GelSight sensor is a vision-based tactile sensor, that measures the 2D texture and 3D topography of the contact target’s surface. It utilizes a piece of elastomeric gel with an opaque coating as the sensing surface, and a webcam above the gel to capture contact deformation from changes in lighting contrast as reflected by the opaque coating. The elastomeric gel is illuminated by color LEDs with inclined angles from different directions. The shading resulting from the inclined lighting is used to reconstruct the 3D geometry of the gel deformation. The original GelSight sensor [14], [15] was designed to measure the 3D topography of the contact surface with micrometer-level spatial resolution but occupied a large space. To integrate the GelSight sensor in a robotic gripper, Li *et al.* [3] designed a cuboid fingertip version. Li’s sensor has a 1×1 cm² sensing area, and can measure fine 2D texture and coarse 3D information of an object’s local surface. A new version of the GelSight sensor was recently proposed by Dong *et al.* [4] to improve the accuracy of 3D geometry measurement and standardize the fabrication process. A detailed review of different versions of GelSight sensors can be found here [16].

GelSight-like sensors with rich 2D and 3D information have been successfully applied in robotic manipulation. Li *et al.* [3] demonstrated its localization capabilities in an automatic USB insertion task, where the sensor used the texture

of the characteristic USB logo to localize its exact position and guide the insertion. Izatt *et al.* [17] explored the use of the 3D point cloud measured by a GelSight sensor in a state estimation filter to find the pose of a grasped object in a peg-in-hole task. Dong *et al.* [4] used the GelSight sensor to detect slip from variations in the 2D texture of the contact surface, in the loop of a robot picking task. The 2D image structure of the output from a GelSight sensor makes it a good fit for the well-developed deep learning architectures in the field of computer vision. GelSight sensors have also been shown to be able to predict grasp stability [18].

C. Durability of tactile sensors

Frictional wear is a common issue for tactile sensors. Contact forces and torques during manipulation are significant and can be harmful to both the sensor surface and its inner structure. Vision-based tactile sensors are specially sensitive to frictional wear, since they rely on the deformation of a soft surface for their sensitivity. These sensors commonly use some form of soft silicone gel, rubber or other soft material as a sensing surface [10], [19], [13], [4].

To enhance the durability of the sensor surface, researchers have investigated using protective skins such as plastic [13], or making the sensing layer easy to replace by involving 3D printing techniques with soft material [19].

Another especially weak spot of vision-based tactile sensors relies on the adhesion between the soft sensing layer and its stronger supporting layer. Most of the sensors discussed above use either silicone tape or rely on the adhesive property of the silicone rubber, which is limiting for practical shear forces involved in picking and lifting objects. The wear effects on these sensors are especially relevant if one attempts to use them in the context of a data-driven/learning approach [13], [18].

Durability is an important factor to evaluate the practicability of the sensor, however, none of the above provide quantitative analysis of their sensor's durability over usage.

III. DESIGN GOALS

In a typical GelSight-like sensor, a clear gel with an opaque outer membrane is illuminated by a light source and read by a camera (Fig. 3). The position of each of these elements depends on the specific requirements of the sensor. Typically, for ease of manufacturing and optical simplicity, the camera is placed in a position where it can look normal to the gel (left of Fig. 3). To reproduce 3D using photometric techniques like Johnson *et al.* do [15], at least three colors of light must be directed across the gel from different directions.

Both of these geometric constraints, the camera placement and the illumination path, are counterproductive to designing slim robot finger integrations. Existing sensor implementations are cuboid. In most manipulation applications, successful grasping requires fingers with the following qualities:

- **Compactness** allows fingers to singulate objects from clutter by squeezing between them or separating them from the environment.

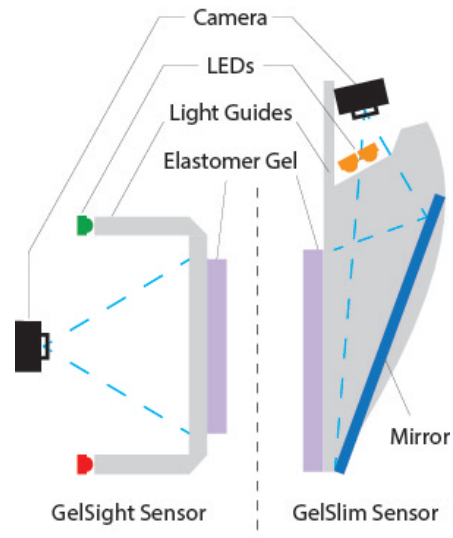


Fig. 3. **The construction of a GelSight sensor.** A general integration of a GelSight sensor in a robot finger requires three components: camera, light, and gel, in particular arrangement. Li's original fingertip schematic [3] is shown at left with ours at right.

- **Uniform Illumination** makes sensor output consistent across as much of the gel pad as possible.
- **Large Sensor Area** extends the spatial-span of the extracted tactile cues, both in the areas where there is and where there is not contact. This can yield improved knowledge of the grasped object's state, and ultimately more controllability.
- **Durability** is necessary for time-span of the tactile information. This is especially important for data-driven techniques that build models from experience.

In this paper we propose a redesign of the form, materials, and processing of the GelSight sensor to turn it into a GelSight *finger*, yielding a more useful finger shape with a more consistent and calibrated output (right of Fig. 3). The following sections describe the geometric and optical tradeoffs in its design (Section IV), as well as the process to calibrate and evaluate it (Section V).

IV. DESIGN AND FABRICATION

To realize the design goals in Section III, we start by re-evaluating the standard design constraints of a vision-based GelSight-like sensor to better match a grasping application: 1) Reactive grasping has less need for precise 3D geometric reconstruction, which simplifies the illumination requirements imposed by photometric stereo. This will reduce the constraints on the light-camera arrangement. 2) The softness of the gel plays a role in the resolution of the sensor, but is also damaging to its life span. We will achieve higher durability by protecting the softest component of the finger, the gel, with textured fabric. 3) Finally, we will improve the finger's compactness, illumination uniformity, and sensor pad size with a complete redesign of the sensor optics from illumination, to gel, to camera.

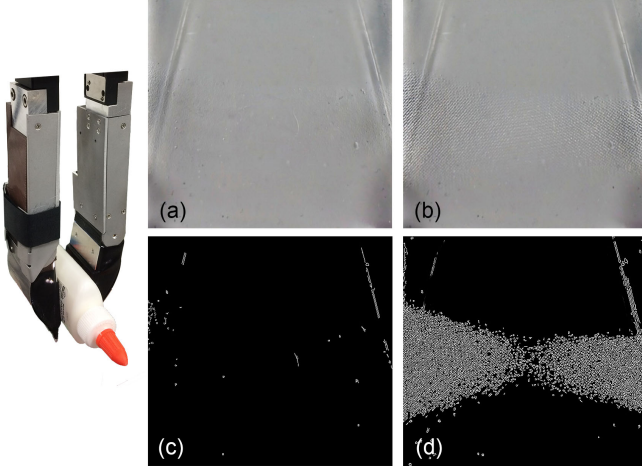


Fig. 4. **Texture in the sensor fabric skin improves signal strength.** (a) When an object with no texture is pushed against the gel with no fabric, signal is very low. (b) The signal improves with textured fabric skin. (c-d) The difference in tactile signal stands out well when processed with Canny edge detection.

A. Gel Materials Selection

To function, a GelSight sensor's gel must be elastomeric, optically clear, soft, and resilient. Gel hardness represents a tradeoff between spatial resolution and strength. Maximum sensitivity and resolution is only possible when gels are very soft, but their softness yields two major drawbacks: low tensile strength, and greater viscoelasticity. Given our application's lesser need for spatial resolution, we were able to make slightly harder, more resilient gels compared to other Gelsight sensors [3], [4]. Our final gel formulation was a two-part silicone (XP-565 from Silicones Inc.) mixed in a 15:1 ratio of parts A to B. The outer surface of our gel was coated with a specular silicone paint using a process developed by Yuan *et al.* [16].

The surface was covered with a stretchy, loose-weave fabric to prevent damage to the gel while also increasing signal strength. Signal strength is proportional to deformation due to pressure on gel surface. Because the patterned texture of the fabric lowers the contact area between target object and gel, pressure is increased to the point where the sensor can detect the contact patch of flat objects pressed against the flat gel (Fig. 4).

B. Sensor Geometry Design Space

Relative to previous GelSight sensors, we improve the sensor's form factor by using a mirror to reflect the gel image back to the camera. This allows us to have a larger sensor pad by placing the camera farther away while also keeping the finger comparatively thin. Thickness of the finger h , shown in Fig. 5 is given by the trigonometric relation:

$$h = \frac{L \cdot \cos(\beta - \frac{\Phi}{2} - 2\alpha)}{\cos(\frac{\Phi}{2} - \beta + \alpha)}, \quad (1)$$

where Φ is the camera's field of view, α is mirror angle, β is the camera angle relative to the base, and L is the length of

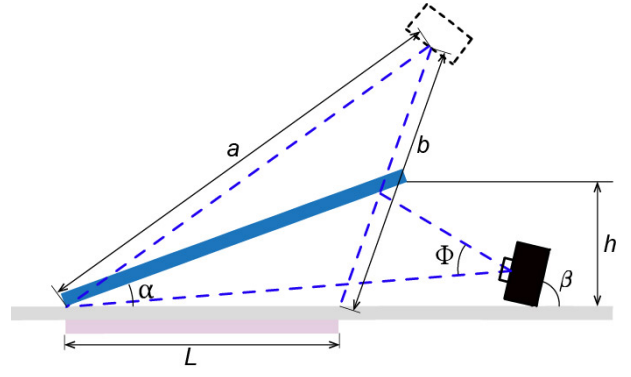


Fig. 5. **The design space of a single-reflection GelSight sensor.** Based on the camera's depth of field and viewing angle, it will lie at some distance away from the gel. Together with mirror and camera angles, these variables play an important role in determining the thickness of the finger and the size of the gel pad. The virtual camera created by the mirror is drawn for visualization purposes.

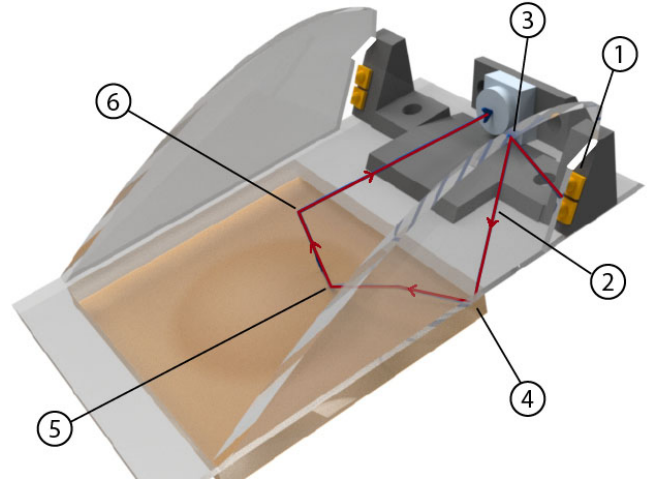


Fig. 6. **The journey of a light ray through the finger.** The red light ray is: 1) Emitted by two compact, high-powered LEDs on each side. 2) Routed internal to acrylic guides via total internal reflection. 3) Redistributed to be parallel and bounced toward the gel pad by a parabolic mirror. 4) Reflected 90° on a mirror surface to graze across the gel. 5) Reflected up by an object touching the gel. 6) Reflected to the camera by a flat mirror (not shown in the figure).

the gel. L is given by the following equation and also relies on the disparity between the shortest and longest light path from the camera (depth of field):

$$L = \frac{(a - b) \cdot \sin \Phi}{2 \sin \frac{\Phi}{2} \cdot \sin(\beta - 2\alpha)}. \quad (2)$$

Together, the design requirements, h and L , are vary with the dependent variables, α and β , and are constrained by the camera's depth of field: $(a - b)$ and viewing angle: Φ . These design equations help to ensure that both near and far edges given by (2) are in focus and that the gel is maximally sized and finger is minimally thick.

C. Optical Path: Photons From Source, to Gel, to Camera

Our method of illuminating the gel makes three major improvements relative to previous sensors: a slimmer finger tip, more even illumination, and a larger gel pad. Much

like Li did in his original GelSight finger design [3], we use acrylic wave guides to move light from source, to gel, to camera with fine control over the angle of incidence across the gel (Fig. 6). However, our design moves the LEDs used for illumination farther back in the finger by using an additional reflection, thus allowing our finger to be slimmer at the tip.

The light cast on the gel originates from a pair of high-powered, surface-mount LEDs (OSLON SSL 80) on each side of the finger. Light rays stay inside the acrylic wave guide because of the total internal reflection phenomenon caused by the difference in refractive index between the acrylic and air. Optimally, light rays would be emitted parallel so as to not lose intensity as light is cast across the gel. However, most light emitters are point sources. Having a line of LEDs, like in Li's sensor, helps to evenly distribute illumination across one dimension, but intensity decays across the length of the sensor.

Our approach uses a parabolic reflection (Step 3 in Fig. 6) to ensure that light rays entering the gel pad are close to parallel. The two small LEDs are approximated as a single point source and placed at the parabola's focus. Parallel light rays then bounce across the gel via a hard 90° reflection. Hard reflections through acrylic wave guides are accomplished by painting those surfaces with mirror finish paint.

When an object makes contact with the fabric over the gel pad, it creates a pattern of high and low spots which correspond to light and dark spots respectively due to the grazing light and specular gel. This image is then transmitted back to the camera off a front-surface glass mirror. The camera (Raspberry Pi Spy Camera) was chosen for its small size, low price, high framerate/resolution, and good depth of field.

D. Packaging and Interfaces

For robotic system integrators, or those interested in designing their own GelSight sensors, the following is a collection of small, but important lessons we learned during our sensor manufacture:

- 1) **Mirror:** Back surface mirrors create a "double image" from reflections off front and back surfaces especially at the reflection angles we use in our sensor. Glass front surface mirrors therefore give better image.
- 2) **Clean acrylic:** Even finger oils on the surface of a wave guide can interrupt total internal reflection. Clean acrylic will prevent low-efficiency illumination.
- 3) **Laser cut acrylic:** Acrylic pieces cut by laser will exhibit stress cracking at edges after contacting any solvent from glue or mirror paint. Cracks break the optical continuity in the substrate and ruin the guide. Stresses can be relieved by annealing first.
- 4) **Gel paint type:** From our experience in this configuration, semi-specular gel coating provides a higher-contrast signal than lambertian gel coatings. Yuan *et al* [16] describe the different types of coatings and how to manufacture them.

- 5) **Affixing silicone gel:** When affixing the silicone gel to the substrate, most adhesives we tried made the images hazy or did not acceptably adhere to either the silicone or substrate. We found that *Adhesives Research ARclear 93495* works well. Our gel-substrate bond is also stronger than other gel-based sensors because of that interface's comparatively large contact area.

Some integration lessons revolve around our use of the use of a raspberry pi spy camera. It enables a very high data-rate but requires a 15-pin Camera Serial Interface (CSI) connection with the raspberry pi. Since this sensor was designed for use on a robotic system where movement and contact are part of normal operation, the processor (raspberry pi) is placed away from the robot manipulator. We extended the camera's fragile ribbon cable by first adapting it to an HDMI cable inside the finger, then passing that HDMI cable along the kinematic chain of the robot. Extending the camera this way allows us to make it arbitrarily long (if thicker cable is used), mechanically and electrically protect the contacts, and route power to the LEDs through the same cable.

The final integration of the sensor in our robot finger also features a rotating joint to change the angle of the finger tip relative to the rest of the finger body. This movement does not affect the optical system, but allows us to more effectively grasp a variety of objects in clutter.

E. Gel Durability Failures

We experimented with several other ways to protect the gel surface before selecting the fabric skin. Most non-silicone coatings will not stick to the silicone bulk so we tested various types of filled and non-filled silicones. Because this skin coats the outside, using filled (tougher, non-transparent) silicones is an option. One thing to note is that thickness added outside of the specular paint increases impedance of the gel, thus decreasing resolution. To deposit a thin layer onto the bulk, we diluted filled, flowable silicone adhesive with NOVOCS silicone thinner from Smooth-On. We found that using solvent in proportions greater than 2:1 (solvent:silicone) caused the gel to wrinkle (possibly because solven difused into the gel and caused expansion).

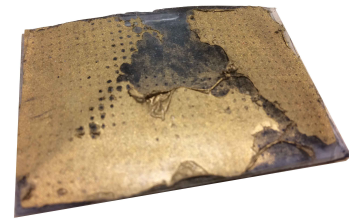


Fig. 7. **Ineffective gel surface treatment.** After just a few hundred grasps, the thin high-toughness silicone coating rubbed off of the gel. In this case, it removed the specular paint with it.

Using a non-solvent based approach to deposit thin layers like spin coating is promising, but we did not explore this path. Furthermore, the thin silicone coatings often rubbed off after just a few hundred grasps, signaling that they did

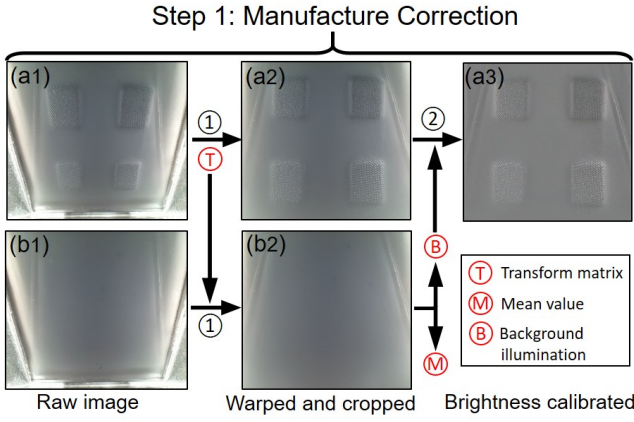


Fig. 8. **Calibration Step 1 (manufacture correction)**: capture raw image (a1) against a calibration pattern with four rectangles and a non-contact image (b1); calculate the “transform matrix” T according to image (a1); do operation ① “image warping and cropping” to image (a1) and (b1) and get (a2) and (b2); apply Gaussian filter to (b2) to get “background illumination” B ; do operation ② to (a2) and get the calibrated image (a3); record the “mean value” M of image (b2) as brightness reference.

not adhere to the gel surface effectively (Fig. 7). Plasma pre-treatment of the silicone surface has potential to more effectively bond substrate and coating, but we were unable to explore this route.

V. SENSOR CALIBRATION

Creating sensor output consistency across individual sensors and over usage are key for sensor usability. The raw image from a GelSlim sensor right after fabrication has two intrinsic issues: non-uniformity in illumination, and strong perspective distortion. In addition, several parameters of the sensor signal may change during use due to small deformations to the hardware, compression of the gel, and camera shutter speed fluctuations. To overcome these problems, we introduce a two-step calibration process, illustrated in Fig. 8 and 9.

Calibration Step 1. Manufacture correction. Right after fabrication, two sensors provide slightly different outcomes due to small changes in camera perspective and illumination. To correct for camera perspective, we capture a tactile imprint against a calibration pattern with four flat squares (Fig. 8 (a1)). With knowledge of the geometry between the corners of the four squares, we estimate the perspective transformation matrix T that allows us to warp the image to normal perspective and crop the boundaries. The output image (Fig. 8 (a2)) contains more user-friendly geometric information about the contact surface. Since the sensor finger tip is rigid, the perspective transformation matrix remains, for the most part, constant after manufacture.

To correct for non-homogenous illumination, we estimate the illumination distribution of the background B by applying a strong Gaussian filter to a non-contact warped image (Fig. 8 (b2)). The output image in Fig. 8 (a3), after subtracting the non-uniform illumination background, is more homogeneous. In addition, we record the mean value of

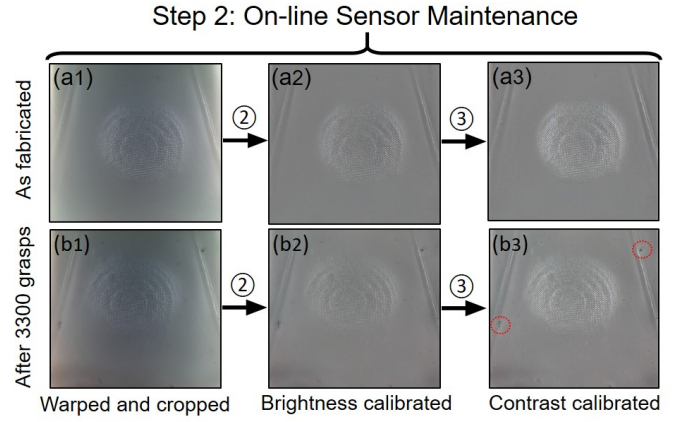


Fig. 9. **Calibration Step 2 (on-line sensor maintenance)**: do operation ① by using T from step one and get warped and cropped (c1) and (d1); do operation ② by using the non-contact image captured at that point and add constant M to keep the brightness and get brightness calibrated (c2) and (d2); do operation ③ “local contrast adjustment” and get contrast calibrated (c3) and (d3). Image (c1)-(c3) and (d1)-(d3) are the “dome” calibration images captured right after fabrication and 3300 grasps, respectively.

the warped non-contact image M as brightness reference for future usage.

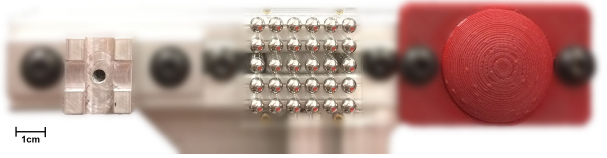


Fig. 10. The three tactile profiles we used to calibrate the sensor. From left to right: A rectangle with sharp corners, a ball-bearing array, and a 3D printed dome.

Calibration Step 2. On-line Sensor Maintenance. The aim of the second calibration step is to keep the sensor output consistent over time. We define four metrics to evaluate the temporal consistency of the 2D signal: *Light intensity and distribution*, *Signal strength*, *Signal strength distribution* and *Gel condition*. We describe and evaluate these metrics in detail in the following subsections.

We track the signal quality with the calibration targets in Fig. 10, including rectangular blocks, a ball-bearing array and a 3D printed dome. We conduct over 3300 grasp-and-lift experiments on several daily objects with two GelSlim fingers on WSG-50 gripper in the robotic system depicted in Fig. 11. We take a tactile imprint of the three calibration targets after every 100 grasps.

A. Metric 1: Light Intensity and Distribution

We define the light intensity and distribution as the mean and standard deviation of the light intensity in a non-contact image. The light intensity distribution in the gel is influenced by the condition of the light source, the consistency of the optical path and the homogeneity of the paint of the gel. The three factors can change due to wear. Fig. 12 shows its evolution versus the number of grasps before (blue) and after (red) background illumination correction. The standard

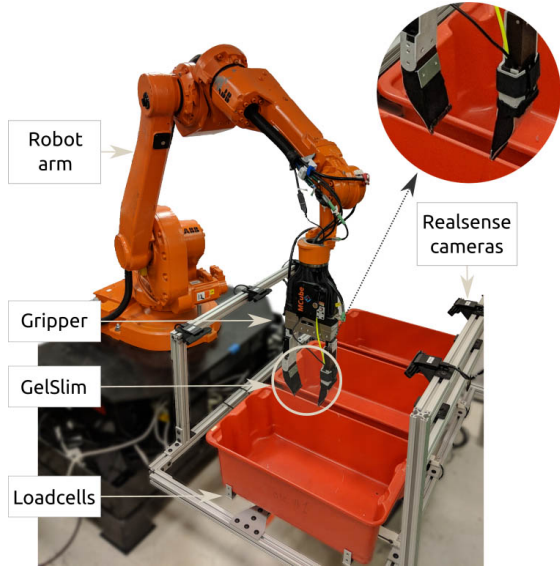


Fig. 11. **The pick-and-place experimental setup.** Our GelSlim fingers are integrated into a gripper on an industrial robot arm that moves household objects between red totes.

deviations are shown as error bars. The blue curve (raw output from the sensor) shows that the mean brightness of the image drops slowly over time, especially after around 1750 grasps. This is likely due to slight damage of the optical path. The variation of the image brightness over space decreases slightly, which is likely caused by the fact that the bright two sides of the image get darker and more similar to the center region. Fig. 9 shows an example of the decrease in illumination before (a1) and after (b1) 3300 grasps.

We compensate for the changes in light intensity by subtracting the background and adding a constant to M (brightness reference from step one) to the whole image. The background illumination is obtained from the Gaussian filtered non-contact image at that point. The mean and variance of the corrected images, shown in red in Fig. 12, are much more consistent. Fig. 9 shows an example of the improvement before (a2) and after (b2) 3300 grasps.

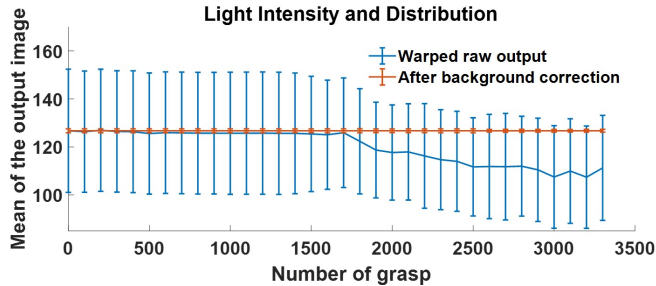


Fig. 12. Evolution of the light intensity distribution.

B. Metric II: Signal Strength

The signal strength S is a measure of the dynamic range of the tactile image under contact. It is intuitively correlated with the brightness and contrast of a contact patch, and we

define it as a function of the mean μ and standard deviation σ of the image intensity restricted to a contact region:

$$S = H(\sigma - m) \left(\frac{2\mu}{255} + \frac{\sigma}{n} \right), \quad (3)$$

where $H(x)$ is the Heaviside step function and $H(\sigma - m)$ means that if the standard deviation is smaller than m , the signal strength is 0. Experimentally, we set m to 5, and n , the standard deviation normalizer, to 30.

Maintaining consistent signal strength during use is one of the most important factors for tactile sensors. In a GelSlim sensor, signal strength is affected by the elasticity of the gel, which degrades after use.

We track the signal strength during grasps by using the “dome” calibration pattern. Fig. 13 shows its evolution. The blue curve representing results from raw output images shows distinct drop of the signal strength after 1750 grasps. The brightness decrease described in the previous subsection is one of the key reasons.

The signal strength can be enhanced by increasing both the contrast and brightness of the image. The brightness adjustment done after fabrication increases the signal strength, shown in green in Fig. 13. However, the image with brightness correction after 3300 grasps shown in Fig. 9 (b2) still has decreased contrast. This explains why the signal strength still drops (in green) with number of grasp.

To enhance the image contrast according to the illumination, we perform adaptive histogram equalization to the image, which increases the contrast on the whole image, and then fuse the images with and without histogram equalization together according to the local background illumination. The two images after the whole calibration are shown in Fig. 9 (a3) and (b3). In addition, the signal strength plot after calibration on illumination and contrast (Fig. 13 in red) shows better consistency over usage.

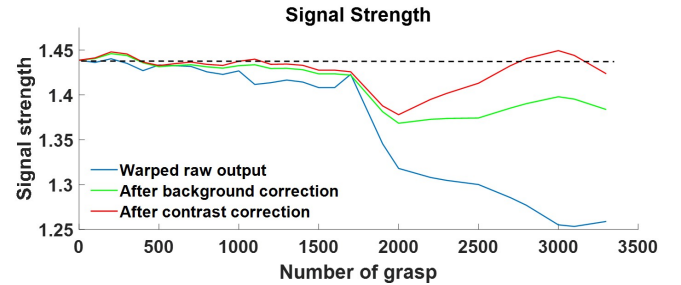


Fig. 13. The change of signal strength across the number of grasp.

C. Metric III: Signal Strength Distribution

When an object is grasped by Gelslim finger, the force distribution on the gel is non-uniform over space. According to our experience, the center region and bottom region of the gel are more likely to be contacted during grasping, which puts more wear on the gel in those areas. This phenomenon results in a non-uniform degradation of the signal strength. To quantify this phenomenon, we extract the signal strength of each pressed region from the “ball array” calibration images (Fig. 14 (b) before and (d) after calibration). We then

use the standard deviation of the 5×5 array to represent the signal strength distribution.

We compensate for variations in signal strength by increasing it non-uniformly in the decreased regions. Fig. 14 shows signal strength distribution before and after calibration in (blue) and (red) respectively. The red curve shows some marginal improvement in the consistency over usage.

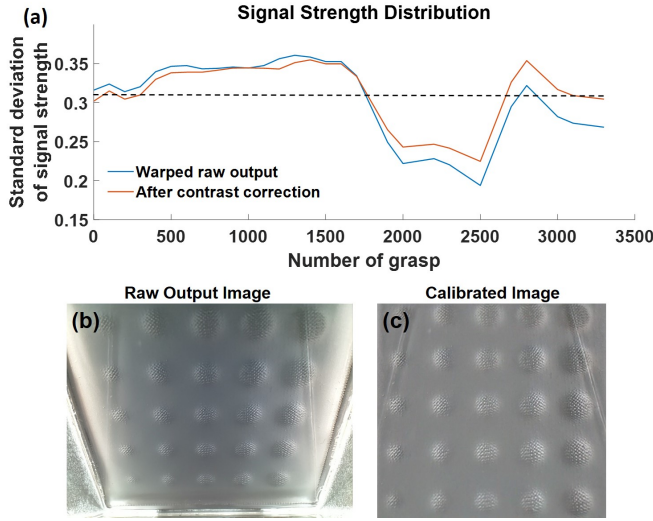


Fig. 14. (a) The evolution of signal strength distribution (b) The raw output of "ball array" calibration image (c) The calibrated "ball array" calibration image.

D. Metric IV: Gel Condition

The sensor's soft gel is covered by a textured fabric skin for protection. Experimentally, this significantly increases the resilience to wear. However, the layer of reflective paint, may still wear out after use. Since the specular paint acts as a reflection surface, a regions of the gel with damaged paint will not respond to contact signal and are seen as black pixels, which we call *dead pixels*.

We define the gel condition as the percentage of dead pixels in the image. Fig. 15 shows the evolution of the number of dead pixels after more than 3000 grasps. The curve shows that only a small amount (less than 0.06%, around 170 pixels) are damaged, for example highlighted with red circles in Fig. 9 (b3).

It is important to note that sparse dead pixels can be ignored or fixed with interpolation, but a large number of clustered dead pixels can only be solved by replacing the gel.

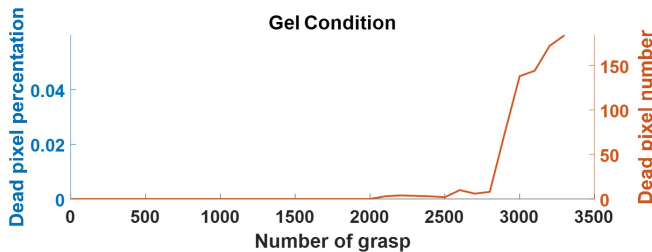


Fig. 15. Evolution of the gel condition.

VI. CONCLUSIONS AND FUTURE WORK

In this paper, we present a solution to the problem of compact integration of visual-tactile sensors in robotic phalanges. Our durable design features: a gel covered with a textured fabric skin that improves durability and contact signal strength; a compact integration of the GelSight sensor optics; and an improved illumination over a large tactile area. Despite the improved wear resistance, the sensor still ages over use. We propose four metrics to track this aging process and created a calibration framework to regularize sensor output over time. We show that, while the sensor degrades minimally over the course of several thousand grasps, the digital calibration procedure is able to condition the sensor output to maintain its youthful glow.

Sensor Function. This sensor outputs a calibrated image that can be used directly in model-based or learning-based approaches to robot grasping and manipulation. For example, if the sensor output is passed through edge detection or morphological filters, areas of the gel in contact with an object can be gleaned. This information could be used to track object pose, inform a data-driven classifier to predict grasp stability, or as real-time observations in a closed-loop regrasp policy. Several of these problems are well aligned with the long term goal to enable reactive grasping and manipulation.

Next steps toward robotic dexterity. The presented solution is just one path toward robust sensors for dexterous robot manipulation control and learning. We have demonstrated the feasibility of a new branch of GelSight sensors without photometric stereo. There are numerous ways to continue improving the sensor's durability and simplify the sensor's fabrication process. For example, while the finger is *slimmer*, it is not *smaller*. It will be a challenge to make integrations sized for smaller robots. Additionally, our finger has an unsensed, rigid tip that is less than ideal for two reasons: it is the part of the finger with the richest contact information, and its rigidity negatively impacts the sensor's durability. Because of the finger's general stiffness, forces increase drastically over small collisions. To decrease this, in the future, we will add compliance to the finger-sensor system. As we create the physical tools necessary for enabling general robotic reactivity and dexterity, future work focuses on using these sensor outputs to learn reactive behaviors so robots can manipulate beyond the laboratory.

REFERENCES

- [1] H. Yousef, M. Boukallel, and K. Althoefer, "Tactile sensing for dexterous in-hand manipulation in roboticsa review," *Sensors and Actuators A: physical*, vol. 167, no. 2, pp. 171–187, 2011.
- [2] C. Chorley, C. Melhuish, T. Pipe, and J. Rossiter, "Development of a tactile sensor based on biologically inspired edge encoding," in *ICAR*. IEEE, 2009, pp. 1–6.
- [3] R. Li, R. Platt, W. Yuan, A. ten Pas, N. Roscup, M. A. Srinivasan, and E. Adelson, "Localization and manipulation of small parts using gelsight tactile sensing," in *IROS*. IEEE, 2014, pp. 3988–3993.
- [4] S. Dong, W. Yuan, and E. Adelson, "Improved gelsight tactile sensor for measuring geometry and slip," *IROS*, 2017.

- [5] N. Correll, K. Bekris, D. Berenson, O. Brock, A. Causo, K. Hauser, K. Okada, A. Rodriguez, J. Romano, and P. Wurman, "Analysis and Observations from the First Amazon Picking Challenge," *T-ASE*, vol. 15, no. 1, pp. 172–188, 2018.
- [6] A. Zeng, K.-T. Yu, S. Song, D. Suo, E. Walker, A. Rodriguez, and J. Xiao, "Multi-view self-supervised deep learning for 6d pose estimation in the amazon picking challenge," in *ICRA*. IEEE, 2017, pp. 1386–1383.
- [7] A. Zeng, S. Song, K.-T. Yu, E. Donlon, F. Hogan, M. Bauza, D. Ma, O. Taylor, M. Liu, E. Romo, N. Fazeli, F. Alet, N. Chavan-Dafle, R. Holladay, I. Morona, P. Q. Nair, D. Green, I. Taylor, W. Liu, T. Funkhouser, and A. Rodriguez, "Robotic pick-and-place of novel objects in clutter with multi-affordance grasping and cross-domain image matching," in *ICRA*. IEEE, 2018.
- [8] R. S. Dahiya, G. Metta, M. Valle, and G. Sandini, "Tactile sensing from humans to humanoids," *IEEE T-RO*, vol. 26, no. 1, pp. 1–20, 2010.
- [9] M. Ohka, Y. Mitsuya, K. Hattori, and I. Higashioka, "Data conversion capability of optical tactile sensor featuring an array of pyramidal projections," in *MFI*. IEEE, 1996, pp. 573–580.
- [10] K. Kamiyama, K. Vlack, T. Mizota, H. Kajimoto, K. Kawakami, and S. Tachi, "Vision-based sensor for real-time measuring of surface traction fields," *CG&A*, vol. 25, no. 1, pp. 68–75, 2005.
- [11] N. J. Ferrier and R. W. Brockett, "Reconstructing the shape of a deformable membrane from image data," *IJRR*, vol. 19, no. 9, pp. 795–816, 2000.
- [12] B. Ward-Cherrier, N. Rojas, and N. F. Lepora, "Model-free precise in-hand manipulation with a 3d-printed tactile gripper," *RA-L*, vol. 2, no. 4, pp. 2056–2063, 2017.
- [13] A. Yamaguchi and C. G. Atkeson, "Combining finger vision and optical tactile sensing: Reducing and handling errors while cutting vegetables," in *Humanoids*. IEEE, 2016, pp. 1045–1051.
- [14] M. K. Johnson and E. Adelson, "Retrographic sensing for the measurement of surface texture and shape," in *CVPR*. IEEE, 2009, pp. 1070–1077.
- [15] M. K. Johnson, F. Cole, A. Raj, and E. H. Adelson, "Microgeometry capture using an elastomeric sensor," in *TOG*, vol. 30, no. 4. ACM, 2011, p. 46.
- [16] W. Yuan, S. Dong, and E. H. Adelson, "Gelsight: High-resolution robot tactile sensors for estimating geometry and force," *Sensors*, vol. 17, no. 12, p. 2762, 2017.
- [17] G. Izatt, G. Mirano, E. Adelson, and R. Tedrake, "Tracking objects with point clouds from vision and touch," in *ICRA*. IEEE, 2017.
- [18] R. Calandra, A. Owens, M. Upadhyaya, W. Yuan, J. Lin, E. H. Adelson, and S. Levine, "The feeling of success: Does touch sensing help predict grasp outcomes?" *arXiv preprint arXiv:1710.05512*, 2017.
- [19] B. Ward-Cherrier, N. Pestell, L. Cramphorn, B. Winstone, M. E. Giannaccini, J. Rossiter, and N. F. Lepora, "The tactip family: Soft optical tactile sensors with 3d-printed biomimetic morphologies," *Soft Robotics*, 2018.